***Original Research Article***

# Sorption Studies of Dyestuffs on Low Cost Adsorbent


## ABSTRACT

This work presents the results of sorption studies of orange G and phenol Red dyes onto palm kernel shell activated carbon (PKS-AC). The adsorbent was prepared by chemical activation using zinc chloride. The effect of various parameters such pH, initial ion concentration, contact time, temperature and adsorbent dosage has been investigated in the present study. The result showed that the percentage removal of dye is concentration dependent, decreasing with an increase in dye concentration. Isotherm modeling was investigated and Freundlich isotherm model fits the equilibrium data very well. The kinetic modeling showed that Pseudo-first order kinetic model best described the kinetics of the adsorption. The thermodynamic parameters were evaluated. The negative values of $\Delta G$ and $\Delta H$ indicate that adsorption process was spontaneous and exothermic. The negative value of $\Delta S$ shows decreased randomness with the adsorption. The study has shown that palm kernel shell activated carbon is a good adsorbent for the removal of phenol red and orange G dyes.


Keywords: Adsorption, isotherm, kinetics, thermodynamics, Palm kernel shell

## INTRODUCTION

The removal of dyes from coloured effluents, particularly from textile industries, is one of the major environmental concerns these days [1]. Many physical and chemical treatment methods including adsorption, coagulation, precipitation, filtration, electro dialysis, membrane separation and oxidation have been used for the treatment of dye- containing effluents [2]. Many problems that have been associated with most of the above methods include high cost, low efficiency, generation of toxic products and inability to regenerate the starting materials [3]. Owing to these problems, emphasis has now been shifted to the use of adsorption for the removal of wastewater pollutants, which is now one of the efficient techniques [4].

Adsorption is a process in which a solid is used for removing a soluble substance from water. It involves the transfer of a mass of a fluid to the surface of an adsorbing solid. The adsorption process has an edge over the other methods due to its sludge free clean operation and complete removal of dyes even from dilute solutions. Activated carbon is the most widely used adsorbent for this purpose because of its extended surface area, microporous structure, high adsorption capacity and high degree of surface reactivity [5]. Some materials that have been used as activated carbon include rice husk, chitin [6], saw dust [7], barley straw and its ash [8], fluted pumpkin [9], Sveta Sariva plant root [10] etc.

But considering the high cost of importing activated carbon and also that a substantial fraction of the activated carbon is lost during each regeneration cycle [11], there is now increase in researches that have been directed towards investigating the adsorption potentials and characteristics of cheaper, effective and efficient adsorbents from natural solid waste materials. Recently, special attention has been focused on the use of low cost adsorbents mainly from agricultural waste products as an alternative to replace the conventional adsorbents [5].

The present investigation reports the use of activated palm kernel shell to adsorb the dyestuffs (phenol red and orange G) from aqueous solution in a batch study.

## MATERIALS AND METHODS

### Adsorbent

The palm kernel shells obtained from Aku (Palm karnel) in Igbo-Etiti Local Government in Enugu State Eastern Province of Nigeria were further dried in the sunlight to reduce the moisture content. The dried material was mixed with $ZnCl_2$ (ratio 1:1) and kept in oven at 383K for 24 hours. Then it was washed severally with distilled water and was leached with warm water to remove any trace of metal. The material was placed in a muffle furnace and the temperature was gradually raised up to 773K and the vessel kept at the same temperature for an hour. After cooling, the material was taken out and ground well by using mortar and pistil and then sieved to particle size of 75µm, preserved in air tight container for further studies on adsorption.

### Adsorbates

The phenol red and orange G used in the present study were procured from Onitsha main market, Nigeria. 0.1 gram of the dye was accurately weighed and made up to 1000ml of distilled water. The structure of the phenol red and orange G are shown in Figures 1 and Figure 2 respectively.

### Characterization of Adsorbent

The physical properties of the carbon before and after activation were determined using standard methods. The ash content and moisture content were determined using ASTM D 28866-70 [12] and ASTMD 2867-70 [13] respectively. The pH was determined using standard test of ASTM D 3838-80 [14]. The surface area was determined using the Sears method [15, 16]. The carbon was also characterized using Scanning Electron Microscopy (SEM) and Fourier Transform Infrared (FTIR) to examine the surface morphology of the carbon and to determine the functional groups present in the carbon respectively.

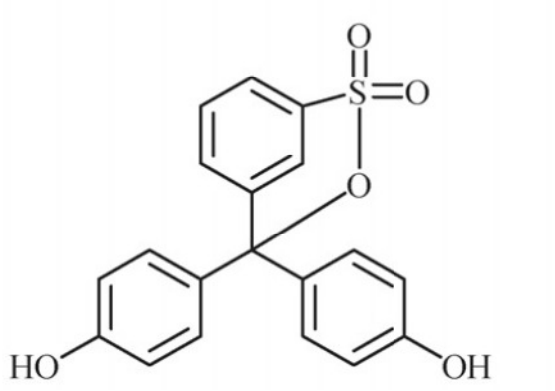


Figure 1. Molecular structure of phenol red.

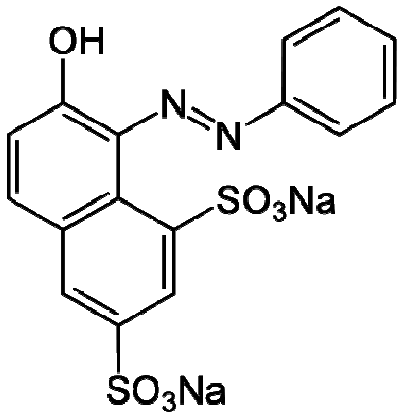


Figure 2. Molecular structure of orange G.

**The Batch Adsorption Studies**

The dye solutions were prepared by dissolving 0.1g of the dyes in 1000ml of distilled water each to get a solution of 100mgL$^{-1}$. After the adsorption, the solution was allowed to settle and the absorbance measured at their respective wavelengths. The amount of equilibrium adsorption, $q_e$ (mgg$^{-1}$) was calculated as given in equation 1.

$$q_e = \frac{(C_o - C_e)V}{m} \quad (1)$$

Where, $C_o$ and $C_e$ (mgL$^{-1}$) are the liquid–phase concentrations of dye at initial and equilibrium respectively. V is the volume of the solution (L) and *m* is the mass of active carbon used (g). The effects of various parameters such as pH, initial ion concentration, contact time, adsorbent dosage and temperature were investigated.

**Isotherm Study**

Isotherm models such as Langmuir and Freundlich models were investigated by using 0.5g of activated carbon at different initial concentration of the dye solution (50-500mgL$^{-1}$) for 60 minutes. Then the final concentration of the dye solution was determined.

**Kinetic Study**

0.5g of the activated carbon was used in 100mg/l of the dye solution at different temperatures (303-333K). The final concentration was determined at a time of 60 minutes. Different kinetic models were applied.

**Thermodynamic Study**

The thermodynamic parameters such as change in free energy (ΔG), enthalpy (ΔH) and entropy (ΔS) can be determined using the following equations:

$$\Delta G = -RT\ln K \quad (2)$$

$$\ln K = \frac{\Delta S}{R} - \frac{\Delta H}{RT} \quad (3)$$

Where R (8.314J/molK) is the general gas constant, T (K) is the absolute temperature and K (Lg$^{-1}$) is the standard thermodynamic equilibrium constant defined as $q_e/C_e$. By plotting a graph of InK versus $T^{-1}$, the values ΔH and ΔS can be estimated from the slopes and intercepts respectively.

**RESULTS AND DISCUSSIONS**

**Physical Properties of the Carbon**

The result of the physical properties of the carbon before and after activation with zinc chloride is shown in Table 1. The result showed that the surface area of the activated carbon was more than the surface area of unactivated carbon. The unactivated palm kernel shell (UPKS) carbon

has a surface area of 192.6$m^2g^{-1}$ while the activated palm kernel shell (PKS-AC) has a surface area of 567$m^2g^{-1}$. This was in corroboration with the range recommended by [17] in their book, that widely used activated carbon adsorbents have specific surface area on the order 500 to 1500 $m^2g^{-1}$. The change in the surface area between activated carbon and unactivated carbon was due to the chemical effect of the activation of the carbon at a given temperature. The activation causes reaction that takes place on all the internal surfaces of the carbons, removing carbon from the pore walls and thereby enlarging them [18].

Table 1. Physical properties of UPKS and PKS-AC.

| **Property** | **UPKS** | **PKS-AC** |
|---|---|---|
| Surface area ($m^2g^{-1}$) | 192.6 | 567 |
| pH | 6.2 | 6.8 |
| Moisture content (%) | 8.2 | 0.51 |
| Ash content (%) | 6.24 | 3.48 |
| Bulk density($g/cm^3$) | 0.48 | 0.8 |

**Characterization of adsorbent using FTIR**

The chemical structure of the adsorbent is of vital importance in understanding the adsorption process. The FTIR technique is an important tool for identifying the characteristic functional groups, which are instrumental in adsorption of organic compounds [19].The FTIR spectra of carbons before and after activation were used to determine the vibrational frequency changes in the functional groups in the adsorbent.

Figure 3 shows the peaks between 3044.6 – 3793.9 $cm^{-1}$ which indicate the existence of free hydroxyl groups, the C-H stretching vibration around (2061.4 – 2905.5 $cm^{-1}$) indicates the presence of alkenes. The peaks (1620.9 – 1716.65 $cm^{-1}$) correspond to the C=O stretching that may be attributed to the hemicellulose and lignin aromatic groups [20]. The C=C stretching vibrations ranging between 1541.12 $cm^{-1}$ and 1697.3 $cm^{-1}$ are indicative of alkenes and aromatic groups [19]. The peaks around 1131.2 to 1399.6 $cm^{-1}$ and 723.17 to 942.55 $cm^{-1}$, correspond to Si -O- Si and Si-H groups respectively.

Palm Kernel Shell Activated Carbon (PKS – AC): Figure 4 shows the FTIR of $ZnCl_2$ activated carbon, where the bands between 3081.5 - 3757.4 $cm^{-1}$ indicate the existence of carboxylic groups [21]. The bands at (2192.1 – 2930.5 $cm^{-1}$), ascribed to C≡C vibration in alkyne groups, which are more intense than the unactivated Palm Kernel Shell at this range is due to release of light volatile matter such as H, resulting from the heat treatment process. [22], reported that the peak between 1283.5 to 1171.8 $cm^{-1}$ may be attributed to the phosphorus-containing group P=O, C-O stretching vibrations in P-O-C linkage. The decrease in band between 3757.5 and 3375.2 $cm^{-1}$ indicate the removal of ash in the carbon.

**Characterization of adsorbent using SEM.** Plate 1 and Plate 2 show the morphological characteristics of UPKS and PKS-AC. The large pores of different shapes could be observed for

the activated carbon. This may be attributed to the fact that the activating agents promote the contact area between the carbon and the activating agent, and therefore, increases the surface area and porosity of carbon. The mechanism for zinc chloride activation tends to produce a well-developed porosity besides high carbon yield, since zinc chloride degrades the cellulose, hemicelluloses and lignin. According to the micrograph, it seems that the cavities on the surfaces resulted from the evaporation of the activating agent during carbonization, leaving the space previously occupied by the activating agent [23].

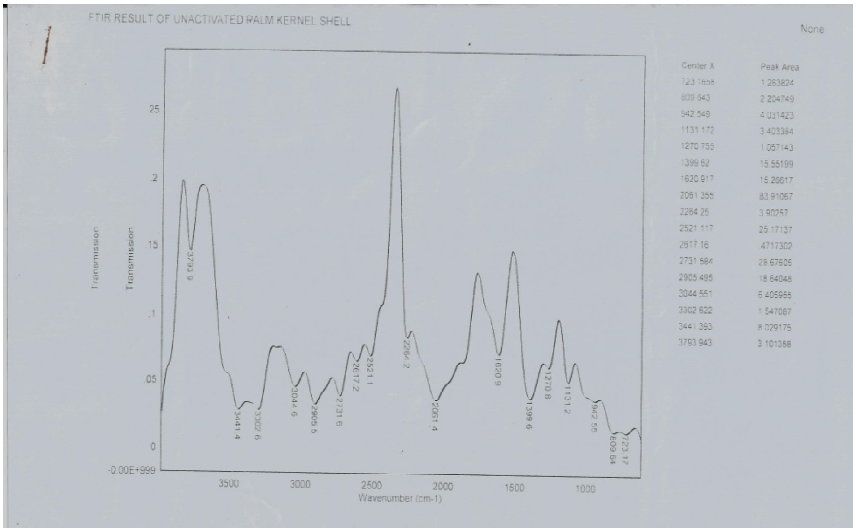


Figure 3. FTIR result of UPKS.

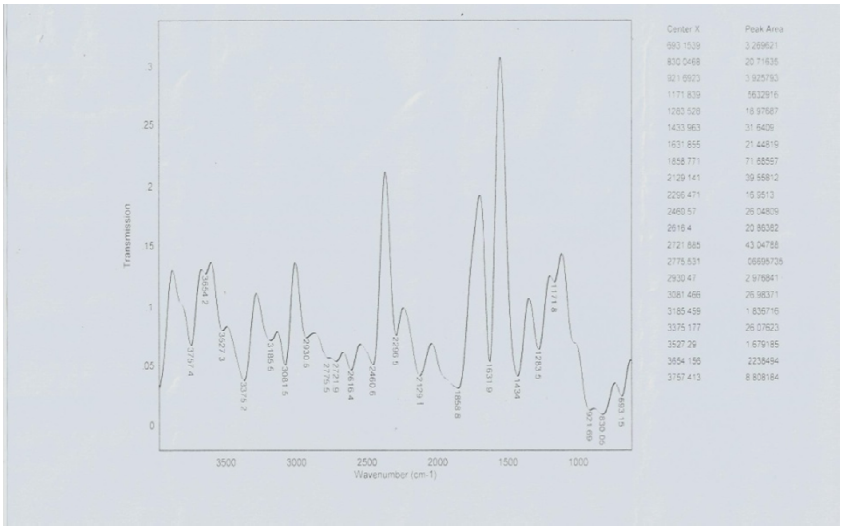


Figure 4. FTIR result of PKS-AC.

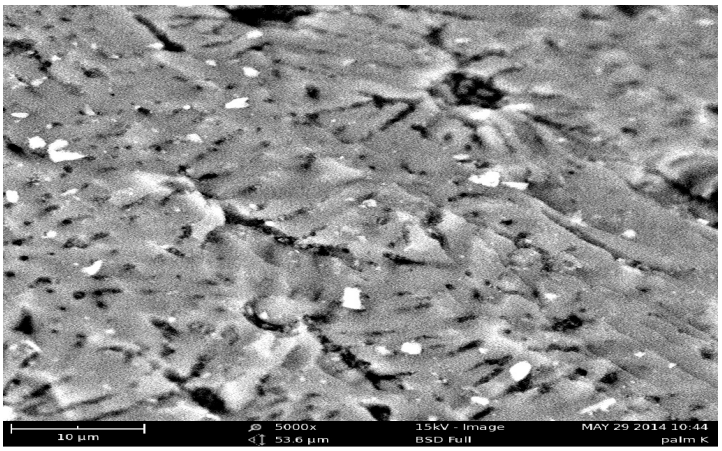


Plate 1. SEM of UPKS at 75µm particle size.

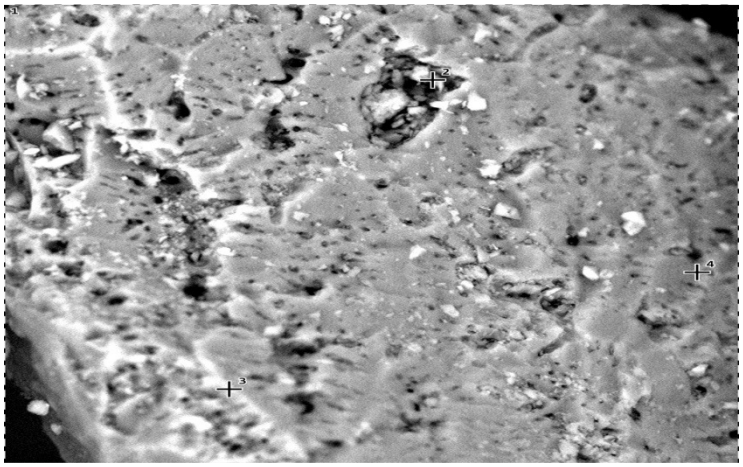

Plate 2. SEM of PKS -AC at 75µm particle size (Mag.= 5000x)

**Adsorption of dyes**

The mechanism of dye adsorption was investigated in the study using different parameters such as pH, initial ion concentration, contact time, temperature and adsorbent dosage.

**Effect of pH**

The percentage of removal of the dyes was studied over the pH range of 2 to 10 as shown in Figure 5. The result showed that for Orange G, the maximum removal occurred at pH of 2 and decreased as the pH increased up to pH 10. This is because at low pH, the degree of protonation of the surface of the activated carbon will be more which will result in increase in diffusion and subsequently increase in adsorption due to electrostatic attraction [24].

For Phenol Red, the percentage removal was found to increase as the pH increased from pH 2 to 8. The lower adsorption of Phenol Red at low pH value was due to the presence of excess $H^+$ ions competing with dye cations for the adsorption sites of the adsorbent. This agrees with [25, 26].

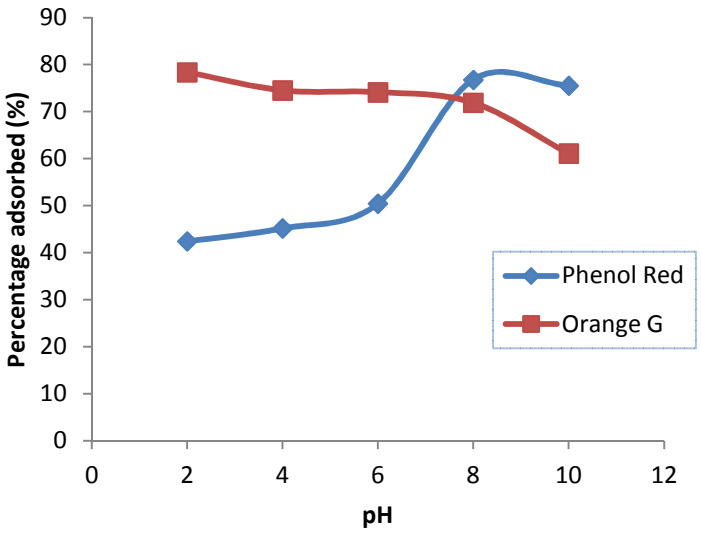


Figure 5.Effect of pH on adsorption of phenol red and orange on PKS-AC.

**Effect of initial concentration at different temperature**

The effect of initial ion concentration was studied for the initial ion concentration ranging from 50 to 500mgL$^{-1}$. The results showed that while the amount of Phenol Red and Orange G adsorbed per unit mass increased with increase in initial ion concentration, the adsorption percentage decreased as shown in Figures 6 and 7. This is because at lower concentration, the ratio of the initial number of the dye molecules to the available surface area was low [27]. This is because for a fixed number of active sites remaining the same, the number of substrates ions accommodated in the interlayer space increased so that the removed ions were decreased. This was in corroboration with [28, 29].

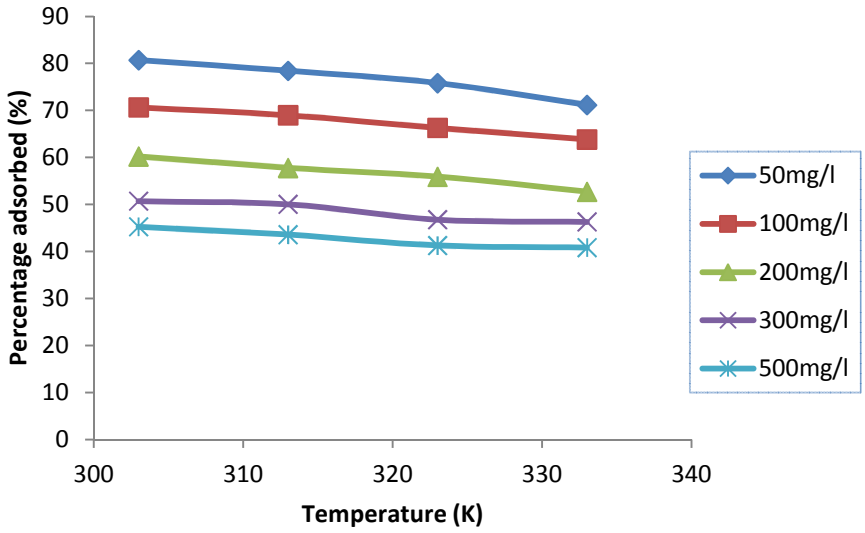


Figure 6. Effect of concentration in the removal of Phenol red by PKS-AC

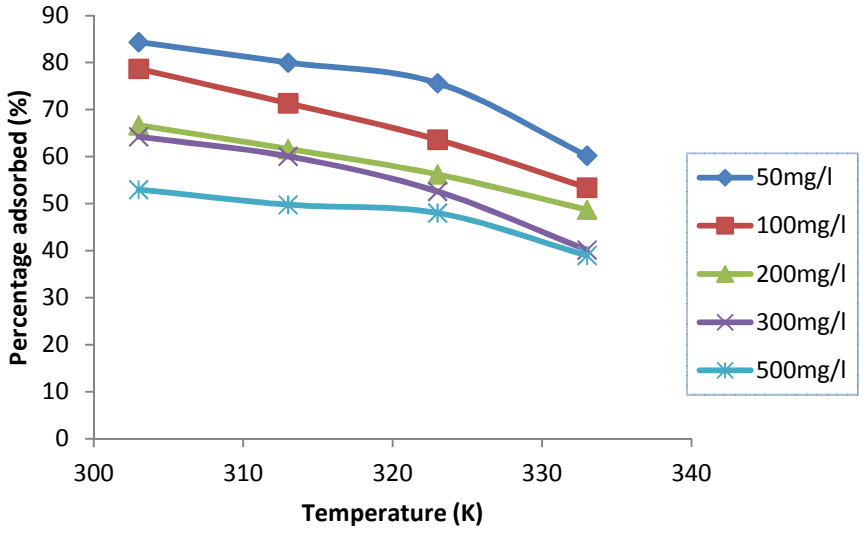


Figure 7. Effect of concentration in the removal of Orange G by PKS-AC

**Effect of contact time**

The result of effect of time on adsorption showed that the removal of dyes increases with increase in agitation time to some extent until equilibrium was reached at about 60mins for both Phenol Red and Orange G as shown in Figures 8 and 9. The initial rapid adsorption was due to the availability of the positively charged surface of the adsorbents for the adsorption of Phenol Red and Orange G [30]. The increase in the extent of removal of the dyes with increasing time was because adsorbate generally formed monolayer on the surface of the adsorbent. Hence, the removal of dyes from aqueous solution was controlled by the rate of the transport of the adsorbate species from the outer sites to the interior sites of adsorbent. This is in agreement with the result obtained by other researchers [31], [32], [33].

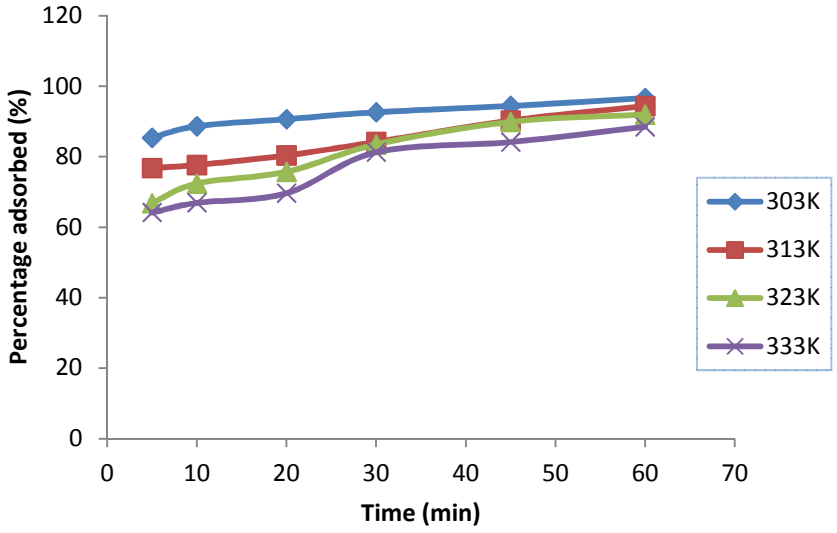


**Figure 8**. Effect of time on adsorption of Phenol Red on PKS-AC.

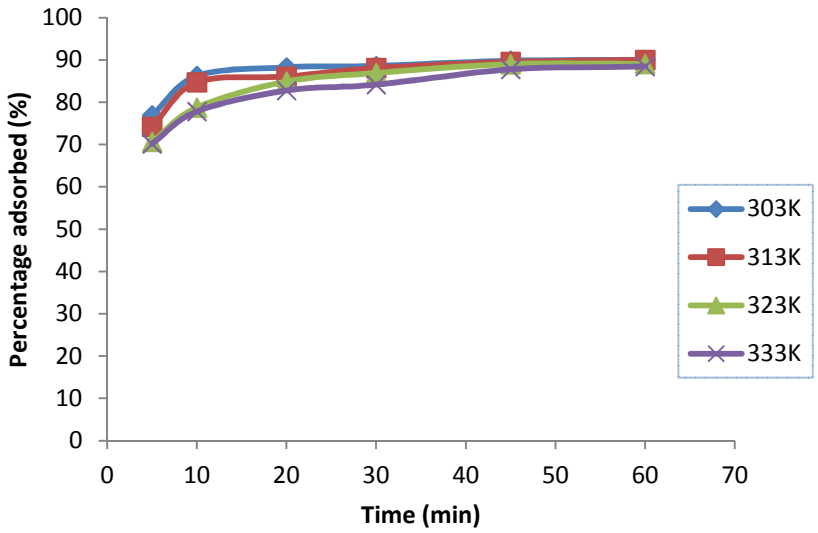


**Figure 9.** Effect of time on adsorption of Orange G on PKS-AC.

**Effect of temperature**

Temperature values ranging from 303K to 333K were used to study the effect of temperature on the adsorption process. It was found out that with increase in temperature, the percentage removal was reduced as shown in Figure 10. This is because as the temperature increases, the rate of diffusion of adsorbate molecules across the external boundary layer and internal pores of the adsorbent particles increases [34]. Temperature affects the rate of removal of dyes by altering the molecular interactions and the solubility of the dyes. Some other researchers reported the same trend [35].

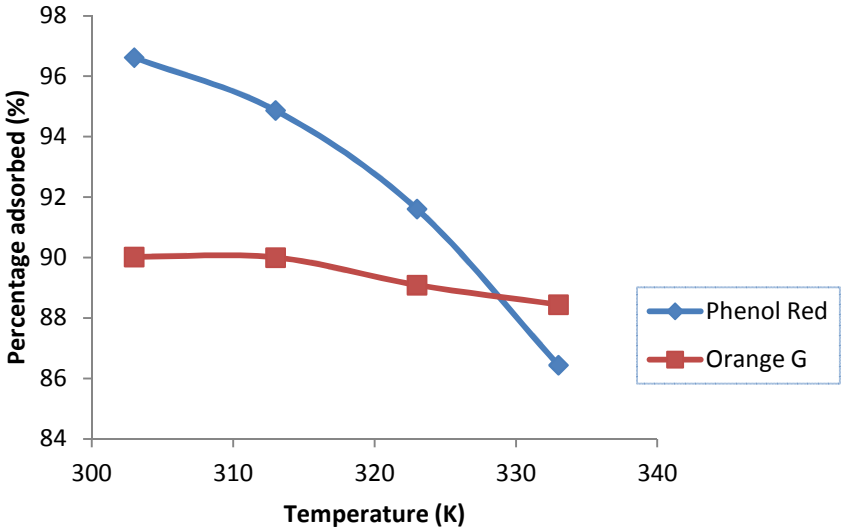


Figure 10. Effect of temperature in the removal of dyes by PKS-AC.

### Effect adsorbent dosage

The effect of dosage was studied for adsorbent dosages in the range of 0.1g to 0.5g. The results showed that, for Phenol Red and Orange G, as the adsorbent dosage increased, the percentage of adsorption also increased as can be seen in Figure 11. The increase in the percentage removal of dyes with the increase in adsorbent dosage was due to the increased surface area with more active functional groups which also gave rise to more availability of more adsorption sites [24, 27]. The decrease in unit adsorption with increasing adsorbent amount was mainly due to adsorption sites remaining saturated during the adsorption reaction [36]. Similar results were obtained by some other researchers [31].

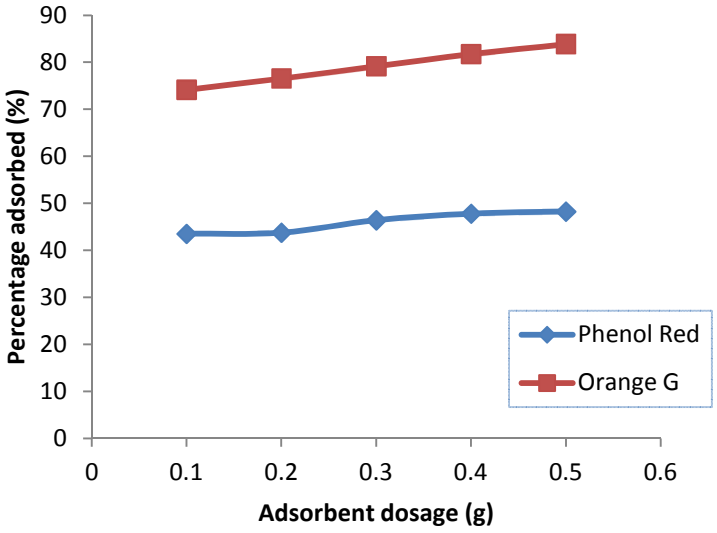


Figure 11. Effect of dosage on adsorption of Phenol Red and Orange G on PKS-AC.

## ADSORPTION ISOTHERM MODELLING

### Langmuir isotherm model

The Langmuir model assumes that the uptake of adsorbate molecules occurs on a homogeneous surface by monolayer adsorption. The linear form of Langmuir isotherm is:

$$\frac{C_e}{q_e} = \frac{1}{bq_m} + \left(\frac{1}{q_m}\right)C_e \qquad (4)$$

Where qe is equilibrium amount of solute adsorbed per unit weight of adsorbent in ($mgg^{-1}$); Ce is equilibrium concentration in aqueous phase ($mgL^{-1}$); $q_m$ is the maximum amount adsorbed per unit mass of adsorbent for a complete monolayer ($mgg^{-1}$); **b** is a constant related to the affinity of the binding sites and energy of adsorption in (l/mg). Hence, plotting the values of 1/qe against 1/Ce, the constants $q_m$ and b were calculated from the intercept and the slope respectively of the linear plot and presented in Tables 2 and 3.

The effect of isotherm shape has been discussed with a view to predicting whether an adsorption system is 'favorable' or 'unfavorable'. A dimensionless separation factor, $R_L$, as an essential feature of the Langmuir isotherm is defined as:

$$R_L = \frac{1}{1 + bC_{ref}} \quad (5)$$

Where, $C_{ref}$ is the reference fluid-phase concentration of adsorbate (mg/l) and **b** is the Langmuir constant. For a single adsorption system, $C_{ref}$ is usually the highest fluid-phase concentration encountered. The value of $R_L$ indicates whether the adsorption isotherm is unfavorable ($R_L>1$), linear ($R_L=1$), favourable ($0<R_L<1$), or irreversible ($R_L=0$). Therefore, the values of $R_L$ were calculated and presented in Tables 4 and 5 respectively. For the adsorption of both Phenol Red and Orange G on the adsorbent, the $R_L$ values were less than 1 and greater than zero showing that the adsorption was favorable.

**Freundlich isotherm model**

The Freundlich isotherm is commonly used to describe adsorption characteristics for heterogeneous surface. Freundlich isotherm can be expressed as Equation 6:

$$q_e = K_F C_e^{1/n} \quad (6)$$

Where, $K_F$ is the constant related to overall adsorption capacity (mg/g); 1/n is the constant related to surface heterogeneity (dimensionless). The plotting of $q_e$ versus $C_e$ helps to determine 1/n and $K_F$ values presented in Tables 2 and 3. The values of the freundlich constants $K_F$ and n were calculated from the intercept and the slope respectively. For beneficial adsorption, the value of n will be between 1 and 10 [24]. In this work, the values of n ranges from 1 to 3 showing beneficial adsorption of Phenol Red and Orange G on the carbon, the correlation coefficient $R^2$ ranges from 0.93 to 0.99 for both Phenol Red and Orange G adsorption indicating that the adsorption followed Freundlich isotherm model very well.

**Temkin isotherm model**

The Temkin isotherm model assumes that the fall in the heat of adsorption is linear rather logarithmic as stated by freundlich [37]. It involves a study of the heat of adsorption and the adsorbent-adsorbate interaction. Temkin isotherm can be expressed as Equation 7:

$$q_e = \frac{RT}{b}\ln A + \frac{RT}{b}\ln C_e \quad (7)$$

Where $\frac{RT}{b} = B$, T is the absolute temperature in K, R is Universal gas constant, 8.314 $J.mol^{-1}.K^{-1}$, and B is related to the heat of adsorption [38]. The constants for Temkin isotherm were determined from the plot of $q_e$ against ln $C_e$ and presented in Tables 2 and 3. The Temkin constant B shows that the heat of adsorption decreases indicating exothermic adsorption [36].

**Dubinin – Radushkevich isotherm model.**

This model involves temperature effects and quite fairly predicts the experimental data over a wide concentration range [39].
The linear form of Dubinin-Radushkevich Isotherm model [37] is:

$$\ln q_e = \ln q_m - \beta\varepsilon^2 \quad (8)$$

Where $q_m$ is the Dubinin-Radushkevich model monolayer capacity (mmol/g), β a constant related to sorption energy, and Ɛ is the Polanyi potential which is related to the equilibrium concentration as follows:

$$\varepsilon = RT\ln\left(1+\frac{1}{C_e}\right) \quad (9)$$

Where, R is the gas constant (8.314 J/mol K) and T is the absolute temperature .The constant β gives the mean free energy, E, of sorption per molecule of the sorbate when it is transferred to the surface of the solid from infinity in the solution and can be computed using the relationship [40].

$$E = \frac{1}{\sqrt{2\beta}} \quad (10)$$

The constants were calculated from the plot of ln $q_e$ versus $\varepsilon^2$ and presented in Table 2 and Table 3. From the values $R^2$ obtained, the result showed that both Phenol Red and Orange G adsorption did not follow Dubinin-Radushkevich Isotherm model well. The results of E obtained greater than 8KJ/mol obtained indicate that the adsorption is predominantly chemisorptions [41].

Table 2. Calculated isotherm Parameters for the Adsorption of phenol Red on PKS-AC

| **Isotherm model** | **Temperature K** | | | |
|---|---|---|---|---|
| | **303** | **313** | **323** | **333** |
| Langmuir | | | | |
| Q ($mgg^{-1}$) | 27.855 | 26.738 | 24.390 | 25.907 |
| b ($Lmg^{-1}$) | 0.0115 | 0.0108 | 0.0104 | 0.0081 |
| $R_L$ | 0.1736 | 0.1849 | 0.1916 | 0.2482 |
| $R^2$ | 0.9372 | 0.9486 | 0.9442 | 0.9382 |
| Freundlich | | | | |
| n | 1.971 | 1.975 | 2.006 | 1.947 |
| $K_f$ ($Lg^{-1}$) | 1.275 | 1.243 | 1.227 | 1.112 |
| $R^2$ | 0.9975 | 0.9988 | 0.9976 | 0.9986 |
| Temkin | | | | |
| b ($Jmg^{-1}$) | 478.19 | 510.60 | 561.76 | 578.87 |
| A ($Lg^{-1}$) | 0.1635 | 0.1646 | 0.1699 | 0.1596 |
| $R^2$ | 0.9264 | 0.9317 | 0.9315 | 0.9260 |
| Dubinin-Radushkevich | | | | |
| $q_D$ ($mgg^{-1}$) | 13.893 | 13.492 | 12.839 | 12.488 |

| | | | | |
|---|---|---|---|---|
| β ($mol^2J^{-2}$) | 2.0 x $10^{-5}$ | 2.0 x $10^{-5}$ | 2.0 x $10^{-5}$ | 2.0 x $10^{-5}$ |
| E ($KJmol^{-1}$) | 158.11 | 158.11 | 158.11 | 158.11 |
| $R^2$ | 0.7002 | 0.7026 | 0.7055 | 0.7037 |

Table 3. Calculated isotherm Parameters for the Adsorption of Orange G on PKS-AC

| **Isotherm model** | **Temperature K 303** | **313** | **323** | **333** |
|---|---|---|---|---|
| Langmuir | | | | |
| Q ($mgg^{-1}$) | 33.898 | 32.573 | 34.247 | 26.110 |
| b ($Lmg^{-1}$) | 0.0133 | 0.0096 | 0.0062 | 0.0048 |
| $R_L$ | 0.1303 | 0.1727 | 0.2455 | 0.2928 |
| $R^2$ | 0.9621 | 0.9406 | 0.8193 | 0.7960 |
| Freundlich | | | | |
| n | 1.8457 | 1.8443 | 1.8399 | 1.8498 |
| $K_f$ ($Lg^{-1}$) | 1.4305 | 1.3295 | 1.2137 | 0.9999 |
| $R^2$ | 0.9947 | 0.9957 | 0.9979 | 0.9988 |
| Temkin | | | | |
| b ($Jmg^{-1}$) | 390.83 | 429.74 | 469.49 | 604.40 |
| A ($Lg^{-1}$) | 0.1862 | 0.1831 | 0.1737 | 0.1786 |
| $R^2$ | 0.9457 | 0.940 | 0.9159 | 0.9201 |
| Dubinin-Radushkevich | | | | |
| $q_D$ ($mgg^{-1}$) | 16.484 | 15.270 | 13.896 | 11.384 |
| β ($mol^2/J^{-2}$) | 2.0 x $10^{-5}$ | 2.0 x $10^{-5}$ | 2.0 x $10^{-5}$ | 2.0 x $10^{-5}$ |
| E ($KJmol^{-1}$) | 158.11 | 158.11 | 158.11 | 158.11 |
| $R^2$ | 0.7292 | 0.7089 | 0.6733 | 0.7049 |

**Isotherm Statistical Analysis for the Batch Adsorption**

The statistical analyses on the isotherm studies are used to determine the best isotherm model for the adsorption. The Root Mean Square Deviation (RMSD), Coefficient of Variance (C.V), Variance and Mean were estimated. The smaller the values of variance and the RMSD, the better the model. Also, by comparing the correlation coefficient, $R^2$ values it can be seen that the Freundlich isotherm model best fitted the data than the other isotherm models. Equally, the isotherm equations obtained from the experimental data are presented in Tables 4 and 5 respectively**.**

**Table 4.** Isotherm statistical analysis for phenol red using PKS –AC.

| Isotherm Model | $R^2$ | Adj $R^2$ | Mean | RMSD | Variance | C.V | Normalised RMSD (%) |
|---|---|---|---|---|---|---|---|
| Langmuir $\frac{C_e}{q_e} = \frac{1}{0.32} + (\frac{1}{27.86})C_e$ | 0.9370 | 0.9160 | 6.994 | 3.963 | 15.71 | 0.5667 | 40.87 |
| Freundlich $\log q_e = \log 1.28 + \left(\frac{1}{1.97}\right) log C_e$ | 0.9980 | 0.9601 | 1.014 | 0.2927 | 0.0857 | 0.2885 | 39.06 |
| Temkin $q_e = \left(\frac{RT}{478.2}\right) ln0.16 + \left(\frac{RT}{478.2}\right) lnC_e$ | 0.9260 | 0.9013 | 12.20 | 7.262 | 52.73 | 0.5954 | 39.04 |
| Dubinin-Radushkevich $lnq_e = ln13.89 - 2\ x\ 10^{-5}\varepsilon^2$ | 0.7002 | 0.6000 | 2.336 | 0.6739 | 0.4541 | 0.2885 | 39.09 |

**Table 5.** Isotherm statistical analysis for Orange G using PKS –AC.

| Isotherm Model | $R^2$ | Adj $R^2$ | Mean | RMSD | Variance | C.V | Normalised RMSD (%) |
|---|---|---|---|---|---|---|---|
| Langmuir $\frac{C_e}{q_e} = \frac{1}{0.451} + (\frac{1}{33.90})C_e$ | 0.962 | 0.9493 | 4.798 | 2.749 | 7.557 | 0.5729 | 39.19 |
| Freundlich $\log q_e = \log 1.43 + \left(\frac{1}{1.846}\right) log C_e$ | 0.995 | 0.9933 | 1.071 | 0.3171 | 0.1006 | 0.2961 | 39.74 |
| Temkin $q_e = \left(\frac{RT}{390.8}\right) ln0.1 + \left(\frac{RT}{390.8}\right) lnC_e$ | 0.946 | 0.9280 | 14.24 | 8.909 | 79.38 | 0.6257 | 39.99 |
| Dubinin-Radushkevich $lnq_e = ln16.48 - 2\ x\ 10^{-5}\varepsilon^2$ | 0.729 | 0.6387 | 2.466 | 0.7302 | 0.5332 | 0.2961 | 39.73 |

## KINETIC ADSORPTION MODELLING

The kinetic models are used to investigate the mechanism of adsorption and the potential rate controlling steps such as mass transport and chemical reaction processes [25]. The First-order, Pseudo-first order and Bhattacharya-Venkobachor kinetic models were used to test the experimental data

### First-order kinetic model.

The first-order rate expression of Lagergren [42] can be given as:

$$-\ln\left(\frac{C_t}{C_o}\right) = k_1 t \qquad (11)$$

Where $C_o$ and $C_t$ are the initial concentration of dye and concentration at a given time t, respectively (mg/l), and $k_1$ is the rate constant of first-order adsorption ($min^{-1}$). The first-order kinetic model was investigated by plotting $-\ln (C_t/C_o)$ against t. The rate constants were calculated from the slope and presented in Tables 6 and 7 together with the values of the correlation coefficient, $R^2$. Save for adsorption of orange G on PKS -AC, which gave $R^2$ values

of less than 0.9, all the others gave $R^2$ values greater than 0.9 showing that the adsorption followed first-order to an extent.

**Pseudo- first order kinetic model.**

The Pseudo- first order rate expression of Lagergren [43] can be expressed as:

$$\log ( q_e - q_t) = \log(q_e) - \frac{k_1}{2.303} t \quad (12)$$

Where $q_e$ and $q_t$ are the adsorption capacity at equilibrium and at time t, respectively ($mgg^{-1}$), $K_1$ is the rate constant of pseudo first-order adsorption ($Lmin^{-1}$).
Plots of log ($q_e - q_t$) against t was used to express the pseudo-first order at different temperatures. The values of the correlation coefficient $R^2$ were shown in Tables 6 and 7 as well as the constants $K_1$ and $q_e$ that were evaluated. It can be seen that for the adsorption of both dyes on the adsorbents, correlation coefficient $R^2$ values were all > 0.9 indicating that the adsorption may have followed the pseudo-first order. But it must be stated that the $q_e$ values calculated were different from the experimental $q_e$. It has been reported that if the values of $q_e$ calculated were not close to the experimental value of $q_e$, the adsorption is assumed not to have followed the kinetic model even if it has a high correlation coefficient, $R^2$ value [44]. Hence, this adsorption did not follow the Pseudo- first order. Some works that followed this trend include [45, 46].

**Bhattacharya-Venkobachor model.**

Bhatta-Venkobachor model [30] is expressed as:

$$\ln(1-U_t) = K_B.t \quad (13)$$

$$U_t = (C_o - C_t)/(C_o - C_e) \quad (14)$$

The effective diffusion coefficient $D_2$, is obtained from the equation:

$$D_2 = \frac{k_B}{\lambda^2} \cdot r^2 \quad (15)$$

Where, **r** is particle radius.

The plot of ln[1 – $U_t$] against **t** was used to investigate the Bhattacharya-Venkobachor model. The values of the rate constant $K_B$ which was obtained from the slope of the linear plot was used to calculate the effective diffusion coefficient $D_2$ and presented in Tables 6 and 7. The Effective diffusion coefficients $D_2$ determined were of the order 2.0 x $10^{-13}$ to 6.0 x $10^{-13}$ $m^2/s$. The correlation coefficient, $R^2$ was (> 0.90) which shows that the adsorption process conformed to the Bhattacharya-Venkobachor model. Similar result was obtained by [31].

Table 6. Calculated kinetic Parameters for the Adsorption of Phenol Red on PKS-AC.

| **Kinetic model** | **Temperature K** | | | |
|---|---|---|---|---|
| | **303** | **313** | **323** | **333** |
| First order | | | | |
| $K_1(min^{-1})$ | 0.0247 | 0.0258 | 0.0268 | 0.0213 |
| $R^2$ | 0.9863 | 0.9616 | 0.9840 | 0.9647 |
| Pseudo first order | | | | |
| $K_1$ ($min^{-1}$) | 0.0389 | 0.0357 | 0.0596 | 0.0463 |
| $q_e$ (mg/g) | 1.285 | 2.444 | 4.008 | 3.451 |
| $R^2$ | 0.9926 | 0.918 | 0.9373 | 0.9369 |
| Bhattacharya-Venkobachor | | | | |
| $K_B$ | -0.0018 | -0.0032 | -0.0045 | -0.0046 |
| $D_2$ ($m^2/s$) | $-2.56 \times 10^{-13}$ | $-4.56 \times 10^{-13}$ | $-6.41 \times 10^{-13}$ | $-6.6 \times 10^{-13}$ |
| $R^2$ | 0.9458 | 0.9919 | 0.9589 | 0.9436 |

Table 7. Calculated kinetic Parameters for the Adsorption of Orange G on PKS-AC.

| **Kinetic model** | **Temperature K** | | | |
|---|---|---|---|---|
| | **303** | **313** | **323** | **333** |
| First order | | | | |
| $K_1(min^{-1})$ | 0.0118 | 0.0141 | 0.0173 | 0.0161 |
| $R^2$ | 0.634 | 0.740 | 0.8356 | 0.8912 |
| Pseudo first order | 0.0924 | 0.0795 | 0.0887 | 0.0161 |
| $K_1$ ($min^{-1}$) | 1.457 | 1.786 | 2.857 | 2.687 |
| $q_e$ (mg/g) | 0.9363 | 0.9579 | 0.9888 | 0.9536 |
| $R^2$ | | | | |
| Bhattacharya-Venkobachor | | | | |
| $K_B$ | -0.0018 | -0.0023 | -0.0031 | -0.003 |
| $D_2$ ($m^2/s$) | $-2.56 \times 10^{-13}$ | $-3.28 \times 10^{-13}$ | $-4.42 \times 10^{-13}$ | $-4.3 \times 10^{-13}$ |
| $R^2$ | 0.5533 | 0.6381 | 0.7542 | 0.8176 |

**Thermodynamic Study**

The mechanism of adsorption was determined through thermodynamic quantities such as change in free energy (ΔG), change in enthalpy (ΔH), and change in entropy (ΔS). The thermodynamic equilibrium constant, K for the sorption was determined from the intercept of the plots of In (qe/Ce) versus qe of langmuir isotherm. Then, the ΔG, ΔH and ΔS are calculated from the Van't Hoff equations shown in equations 2 and 3. The thermodynamic parameters were calculated from the values of the thermodynamic equilibrium constant, K by plotting of In K versus 1/T. Then the slope and intercept were used to determine ΔH and ΔS, and the Van't Hoff Equation (Equation 2) was applied to calculate ΔG. The values of ΔH, ΔS and ΔG are given in Tables 8 and 9 respectively.

The negative values of ΔG indicate the feasibility of the adsorption process at room temperature and also the spontaneity of adsorption reaction [30]. The negative values of ΔH indicate the exothermic nature of the adsorption in accord with the decreasing adsorption capacity associated with increasing adsorption temperature. This also confirms the possibility of physical adsorption as with the increase in temperature of the system [47]. The negative value of ΔS means the decreased randomness with adsorption of the dyes on PKS -AC [48]. This is because the number of water molecules surrounding the dyes increased during the adsorption process and thus, the degree of freedom of the water molecules decreased indicating that the degree of randomness at the solid-solution interface of the adsorption decreased [49].

Table 8. Thermodynamics parameters for the adsorption of Phenol Red on the adsorbents

| **Adsorbent** | **T (K)** | **ΔG (KJ/mol)** | **ΔS (J/mol K)** | **ΔH (KJ/mol)** |
|---|---|---|---|---|
| PKS -AC | | | | |
| | 303 | -6.153 | | |
| | 318 | -6.192 | -9.206 | -9.033 |
| | 323 | -6.289 | | |
| | 333 | -5.791 | | |

Table 9. Thermodynamics parameters for the adsorption of Orange G on the adsorbents

| **Adsorbent** | **T (K)** | **ΔG (KJ/mol)** | **ΔS (J/mol K)** | **ΔH (KJ/mol)** |
|---|---|---|---|---|
| PKS -AC | | | | |
| | 303 | -6.556 | | |
| | 318 | -5.886 | -29.72 | -29.72 |
| | 323 | -4.900 | | |
| | 333 | -4.343 | | |

**Activation Energy**

The activation energy of adsorption was calculated from the linearized Arrhenius equation:

$$\ln K = \ln A - \frac{E_a}{RT} \qquad (16)$$

Where A is the frequency factor (g/mg.min), K = rate constant value for Second-order kinetics (g/mg.min). $E_a$ = activation energy in $kJmol^{-1}$. T is temperature (K) and R is the gas constant = $8.314KJmol^{-1}.K^{-1}$.The value of $E_a$ can be calculated by the slope of graph 'lnK versus 1/T'. The activation energies from the present system are **-**32.712 $KJmol^{-1}$and -24.787 $KJmol^{-1}$ for phenol red and orange G respectively. The values were in corroboration to the values obtained by [50].

## CONCLUSIONS

The palm kernel shell activated carbon adsorbent has shown to be effective for the removal of phenol red and orange G dyes from aqueous solutions. Adsorption parameters such as pH, initial ion concentration, contacts time, temperature and adsorbent dosage have effect on the adsorption performance of palm kernel shell activated carbon for the removal of dye from wastewater. The isotherm models have been investigated and Freundlich isotherm fitted the equilibrium data. Similarly, the Pseudo-first order kinetic model fitted very with the dynamical adsorption behavior of the dyes. The thermodynamic studies showed that ΔG and ΔH were negative at different temperatures, indicating that the adsorption process is spontaneous and exothermic. The negative value of ΔS shows decreased randomness with adsorption of dye. It may be concluded that PKS-AC can be effectively employed for the removal of the dystuffs in aqueous solutions.

## REFERENCES

1. Wu F.C., Tseng R. L., Juang R. S., Adsorption of dyes and phenols from water on the activated carbons prepared from corncob wastes, Environ technol, 22, 2001, 205 – 13.
2. Robinson T., McMullan G., Marchant R., Nigam P., Remediation of dyes in textile effluent: a critical review on current treatment technologies with a proposed alternative, Bioresource Technology, 77, 2001, 247–255.
3. Ehssan N., Yehia E., Adsorption of Phenol from Aqueous Solution by Local Egyptian Bentonite, American Journal of Science 8(8), 2012, 1-9.

4. Sunil K., Gunasekar V., Ponnusami V., Removal of methylene blue from aqueous effluent using fixed bed of groundnut shell powder, Hindawi Publishing Corporation Journal of Chemistry, 1, 2012, 1-5.
5. Al-Sultani K.F, Al-Seroury F.A, Charactrization of the Removal of Phenol from Aqueous Solution Fluidized Bed Column by Rice Husk Adsorbent, Research Journal of Recent Sciences, 1, 2011,145-151.
6. Omar H. A., Adsorptive removal of phenol from aqueous solution using natural immobilized Chitin by Diathiazone, New York Science Journal, 5(8), 2012, 1-9.
7. Nestor T., Natalia M., Fabiana M., Javier P., Carina P., Tomas C., Phenol adsorption onto powdered and granular activated carbon, prepared from eucalyptus wood, Journal of Colloid and Interface Science, 279, 2004, 357-363.
8. Afshin M., Amir H., Mahvi R. E., Jamil K., Evaluation of Barley Straw and its Ash in Removal of Phenol from Aqueous System, World Applied Sciences Journal, 8(3), 2010, 369-373.
9. Ekpette O. A., Horsfall J. M., Kinetic sorption study of phenol onto activated carbon derived from fluted pumpkin stem waste, ARPN Journal of Engineering and Applied science, 6(6), 2011, 43-49.
10. Srihari V., Ashutosh D., Adsorption of phenol from aqueous media by an Agro-waste (Hemidesmus Indicus) based activated carbon, Applied Ecology and Enivronmental research, 7(1), 2009, 13-23.
11. Sofia A., Tzayhri G., Guillermo O., Del Socorro L., Brenda G., Adsorption of Phenol and Dichlorophenols from Aqueous Solutions by Porous Clay Heterostructure (PCH), J. Mex. Chem. Soc., 49(3), 2005, 287-291.

12. Total Ash Content of Activated Carbon, The Annual book of ASTM standards; copy right, ASTM, Race Street, Philadelphia.PA.1986, 19103.
13. Moisture Content of Activated Carbon, The Annual book of ASTM standards, copy right, ASTM, Race Street, Philadelphia.PA.1986, 19103.
14. pH of Activated Carbon, The Annual book of ASTM standards, copy right, ASTM, Race Street, Philadelphia.PA.1996, 19103.
15. Alzaydian A. S., Adsorption of methylene blue from aqueous solution onto a low cost natural Jordanian clay, American Journal of Applied Sci., 6(6), 2009, 1047-1058.
16. Al-Qadah Z., Shawabkah R., Production and characterization of granular activated carbon from activated sludge, Braz. Journal of Chemical engineering, 26(1), 2009, 6-17.
17. Roop C., Bansal M. G., Activated Carbon Adsorption, Taylor and Francis group, *LLC*, 2005, pp. 1 – 10.
18. Elwood V. R., Process Water Treatment Carbons for Barnebey & Suitcliffe Corporation, Columbus, Ohio, 2000.
19. Cherifi H., Haninia S., Bentahar F., Adsorption of phenol from wastewater using Vegetal cords as a new adsorbent, Desalination, 244, 2009, 177-187.
20. Safa Y., Bhatti H.N., Adsorptive Removal of Direct Dyes by Low Cost Rice Husk, Effect of Treatments and Modification, African Journal of Biotechnology, 10(16), 2011, 28 – 3142.
21. Prahas D., Kartika Y., Indraswati N., Ismadji S., Activated carbon from jackfruit peel waste by H3PO4 chemical activation: Pore structure and surface chemistry characterization, Chemical Eng. Journal 140, 2008, 32–42.

22. Puizy A.M., Poddubnaya O.I., A. Martınez-Alonso A., Sua´rez-Garcı´a F., Tasco´n J.M.D., Synthetic carbons activated with phosphoric acid I.Surface chemistry and ion bonding properties, Carbon, 40, 2002, 1493–505.

23. Devarly P., Kartika Y., Indraswati N., Ismadji S., Activated carbon from jackfruit peel waste by H3PO4 chemical activation: Pore structure and surface chemistry characterization,Chem.Eng.Journal, 140, 2008, 32–42.

24. Ladhe U. V., Wankhede S. K., Patil V. T., Patil P. R., Adsorption of eriochrome black-T from aqueous solutions on activated carbon prepared from mosambi peel, Journal of Applied Sciences in Environmental Sanitation, 6(2), 2011, 149-154.

25. Rajeshkannan R., Rajasimman M., Rajamohan N., Decolourisation of malachite green using tamarind seed: Optimisation, isotherm and kinetic studies, Chemical Industry and Chemical Engineering Quarterly, 17(1), 2011, 67-79.

26. Venckatesh R., Amudha T., Rajeshwari S., Chandramohan M., Jambulingam M., Kinetics and equilibrium studies of adsorption of direct red-28 onto Punica granatum carbon, International journal of engineering and technology, 2(6), 2010, 2040-2050

27. Arivoli S., Hema M., Martin P. D., Adsorption of malachite green onto carbon prepared from borassus bark, The Arabian Journal for Science and Engineering, 34(2A), 2009, 31-43.

28. Shirsath D. S., Shrivastava V. S., Removal of hazardous dye ponceaus by using chitin: an organic bioadsorbent, African journal of environment science and technology, 6(2), 2012, 115-124.

29. Gaikwad R.W., Misal S. A., Sorption studies of methylene blue on silica gel, International Journal of chemical engineering and application, 1(4), 2010, 111-115.

30. Goswami S., Ghosh U. C., Studies on adsorption behavior of Cr (VI) onto synthetic hydrous stanniz oxide, Water *S A*, 31(4), 2005, 597-602.

31. Vikrant V.K., Deshmukh S.K., Kinetic parameters and evaluation performance for decolorization using low cost adsorbent, International conference on future environment and energy, 28, 2012, 95-99.

32. Tabrez A.K., Singh V., Kumar D., Removal of some basic dyes from artificial textile wastewater by adsorption on Akash Kinari coal, Journal of scientific and Industrial Research, 63, 2004, 353-364.

33. Verma V.K., Mishra A.K., Kinetic and isotherm modeling of adsorption of dyes onto rice husk carbon, Global Nest Journal, 10(10), 2010, 1-7.

34. Shahwan T., Erten H.N., Thermodynamics parameters of $Cs^+$ sorption on natural clays, Journal of Radioanalytical and Nuclear Chemistry, 253(1), 2002, 115-120.

35. Rashmi S., Bhattacharya B., Adsorption-coagulation for the decolorisation of textile dye solutions, Water Qual. Res. J. Canada, 38(3), 2003, 553-562.

36. Bulut Y., Aydin H., A Kinetic and Thermodynamic study of methylene blue adsorption on wheat shells, Journal of Desalination, 194, 2006, 259-267.

37. Sivakumar P., Palanisamy P. N., Adsorption Studies of basic red 29 by a non conventional activated carbon prepared from Euphorbia Antiquorum, International Journal Of Chem. Tec. Research, 1(3), 2009, 502-510.

38. Allen S. J, McKay G, Porter J. F., J. Colloid interface sci., 280, 2004, 322 – 333.

39. Inglezakis V.J., Poulopoulos S.G., Adsorption ion exchange and catalysis, Design of Operation and Experimental Applications, 1st edition, Elsevier Publishers, Amsterdam, 16(17), 2006, 66-75.

40. Lin S.H., Juang R.S., Heavy metal removal from water by sorption using surfactant-modified montmorillonite, Journal of Hazard Materials, 92, 2002, 315-326.

41. Arh-Hwang C., Yao-Yi H., Adsorption of Remazol Black 5 from aqueous solution by the template crosslinked-chitosans, Journal of Hazardous Material, 177, 2010, 668-675.

42. Annadurai, Krishnan, Batch kinetic studies of adsorption of reactive dye using chitosan, Indian J. of envivron. Protection, 17(5), 1997, 328 – 333.

43. Maniatis K., Nurmala M., Activated carbon produced from biomass, Biomass Energy Ind. Environ., 274, 1992, 1034 – 1308.

44. Muhammad J. I., Muhammad N.A., Thermodynamics and kinetics of adsorption of dyes from aqueous media onto alumina, Journal Chem. Soc. Pak, 32(4), 2010, 419-428.

45. Xiangliang P., Daoyong Z., Removal malachite green from water by firmiana simplex wood fiber, Electronic Journal of Biotechnology, 12(4), 2009, 1-10.

46. Ozer G., Safa A. O., Adnan O., Adsorption kinetics of naphthalene onto organo-sepiolite from aqueous solutions, Elsevier on Desalination, 220, 2008, 96-107.

47. Sharma Y. C., Singh B., Uma, Fast removal of malachite green by adsorption on rice husk activated carbon, The Open Environment Pollution and Toxicology Journal, 1, 2009, 74-78.

48. Pragnesh N. D., Satindar K., Ekta K., Removal of eriochrome black-T by adsorption onto eucalyptus bark using green technology, Indian Journal of Chemical Technology 18, 2011, 53-60.

49. Muhammad J.I., Muhammad N. A., Adsorption of dyes from aqueous solutions on activated charcoal, Elsevier B. V. 6(7), 2006, 1-11.

50. Jiwan S., Sushmita B., Deepak G., Yogesh C. S., Equilibrium Modeling and Thermodynamics of removal of orange G from its aqueous solutions. Journal of Applied Sciences in Environmental Sanitation, 6(3), 2011, 317 – 326.